



Texture analysis of [^{18}F]-fluorodeoxyglucose-positron emission tomography/computed tomography for predicting the treatment response of postoperative recurrent or metastatic oral squamous cell carcinoma treated with cetuximab

Mai Kim¹ · Wenchao Gu² · Takahito Nakajima^{2,3} · Tetsuya Higuchi² · Masaru Ogawa¹ · Takahiro Shimizu¹ · Takahiro Yamaguchi¹ · Ayako Takahashi² · Yoshito Tsushima² · Satoshi Yokoo¹

Received: 27 February 2021 / Accepted: 29 April 2021 / Published online: 20 May 2021
© The Japanese Society of Nuclear Medicine 2021

Abstract

Objective To assess the value of the texture analysis of fluorine- ^{18}F -fluorodeoxyglucose-positron emission tomography/computed tomography (^{18}F -FDG-PET/CT) in predicting the treatment response of postoperative recurrent or metastatic oral squamous cell carcinoma (POR/M-OSCC) treated with cetuximab.

Methods A total of 14 patients undergoing ^{18}F -FDG-PET/CT with POR/M-OSCC were divided into the responder and non-responder groups according to cetuximab response by Response Evaluation Criteria in Solid Tumors (RECIST). The regions of interest (ROI) were set at the POR/M-OSCC lesions with the highest uptake of ^{18}F -FDG, and the volumetric and texture features were analyzed. The features with correlation coefficient of 0.6 or more were further evaluated using the logistic regression analysis to create a model.

Results The $\text{SHAPE}_{\text{Volume}(\text{vx})}$, $\text{SHAPE}_{\text{Volume}(\text{mL})}$, metabolic tumor volume (MTV), and gray-level run-length matrix run-length nonuniformity ($\text{GLRLM}_{\text{RLNU}}$) were significantly different between the responder ($n=6$) and non-responder ($n=8$) groups ($p=0.044$, 0.042 , 0.047 , and 0.012 , respectively). The model's area under the curve (AUC) was found to be 0.83, 0.83, 0.79, and 0.92, respectively. The heatmap with PET feature dendrogram showed four distinct clusters including them in patient's responder and non-responder groups.

Conclusions Higher MTV, $\text{GLRLM}_{\text{RLNU}}$, $\text{SHAPE}_{\text{Volume}(\text{vx})}$, and $\text{SHAPE}_{\text{Volume}(\text{mL})}$ in ^{18}F -FDG-PET images may have the prediction values for treatment response with POR/M-OSCC treated with cetuximab.

Keywords Postoperative recurrent or metastatic oral cancer · Positron emission tomography image · Metabolic tumor volume · Texture analysis

Mai Kim and Wenchao Gu contributed equally to this manuscript.

✉ Takahito Nakajima
nakajima@md.tsukuba.ac.jp

¹ Department of Oral and Maxillofacial Surgery, and Plastic Surgery, Gunma University Graduate School of Medicine, Maebashi, Japan

² Department of Diagnostic Radiology and Nuclear Medicine, Gunma University Graduate School of Medicine, Maebashi, Japan

³ Department of Diagnostic and Interventional Radiology, University of Tsukuba Hospital, Ibaraki, Japan

Introduction

Approximately 90% of patients with oral cancer were diagnosed with oral squamous cell carcinoma (OSCC), and surgery is the first-line treatment for them [1]. In case of recurrent or metastatic lesions, the standard systemic chemotherapy is considered.

Cetuximab is an epidermal growth factor (EGFR) inhibitor, which is used in the treatment of metastatic colon cancer, metastatic non-small cell lung cancer, and head and neck cancers. EGFR-expressing tumors have been considered as good candidates for this molecular-targeted therapy; however, studies have shown that immunohistochemical EGFR receptor status does not predict the response to cetuximab

treatment [2]. In addition, cetuximab may cause severe adverse effects (such as interstitial pneumonia and severe skin symptoms) which may sometimes be fatal. Therefore, identification of prognostic biomarkers that can predict the tumor response to this therapy is imperative [3–6]. Hoffmann et al. described the response evaluation of innovative approaches, including immune infiltrate, molecular characterization, and functional imaging [7].

Cancer development and progression are characterized by various cancer-specific metabolic abnormalities [8, 9]. Positron emission tomography (PET) using ^{18}F -fluorodeoxyglucose (FDG) is useful not only for tumor detection and staging, but also for detection of recurrence, based on the accelerated glycolysis metabolism of cancer cells. Metabolic tumor volume (MTV) and total lesion glycolysis (TLG), which are determined on FDG-PET, were shown to be associated with or predict the prognosis of patients [10]. However, solid tumor heterogeneity, as assessed by FDG-PET markers, has not been shown to be associated with therapeutic or antitumor efficacy [11].

The purpose of this study was to evaluate the potential of the texture analysis of ^{18}F -FDG-PET/CT in predicting the treatment response to postoperative recurrent or metastatic oral squamous cell carcinoma (POR/M-OSCC) undergoing cetuximab therapy.

Materials and methods

Patients and study characteristics

A total of 68 patients with POR/M-OSCC, who underwent surgery for first line and followed up from December 2013 to January 2020, were selected. All patients were diagnosed by pathological examination of the primary tumors and were found to have postoperative recurrent or metastatic lesions during clinical follow-up. The diagnosis of POR/M-OSCC was confirmed by various imaging examinations and/or clinical examinations. Out of the 18 patients treated with cetuximab, we focused on 14 patients, who underwent ^{18}F -FDG-PET/CT imaging before treatment (Fig. 1). This retrospective study protocol was approved by the Ethics Committee of our institute, and based on the tenets of the Helsinki Declaration. The enrolled patients' agreement was obtained using an opt-out method.

^{18}F -FDG-PET/CT imaging

^{18}F -FDG-PET/CT examinations were performed using GE Discovery ST8 (GE, Milwaukee) or Bio-graph 16 (Siemens Medical Solutions Inc., Malvern, PA). ^{18}F -FDG (5.0 MBq/kg) was intravenously administered after at least 6 h of fasting, and PET/CT imaging was performed 60 min after

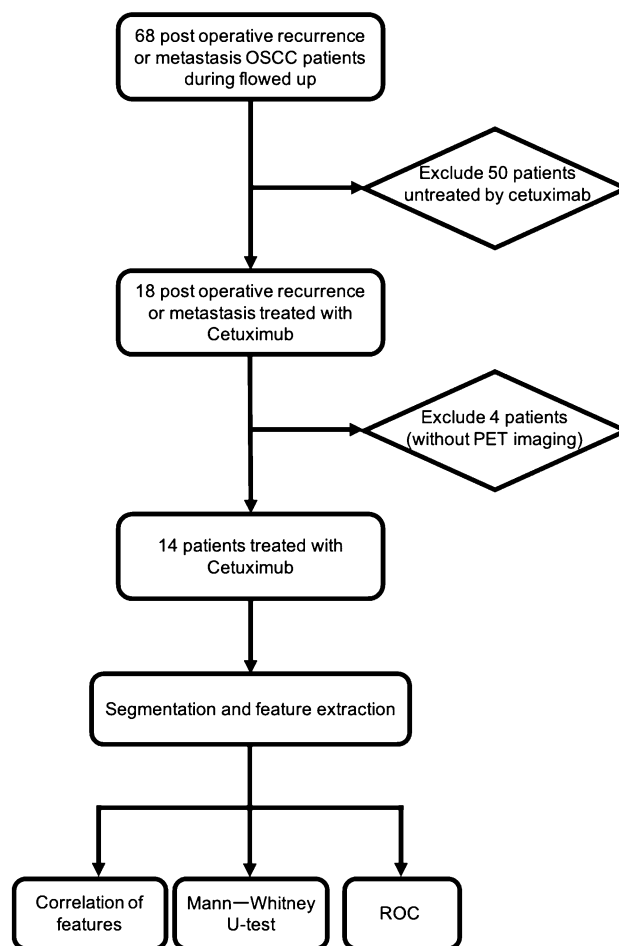


Fig. 1 Flow diagram of patient inclusion, with reasons for exclusion, total study population, and statistical analysis

administration of ^{18}F -FDG. The segmented attenuation correction was performed using CT (140 kV, 120–240 mAs) to produce 128×128 matrix images.

Texture analysis

Segmentations of POR/M-OSCC lesion segmentation on all FDG-PET were performed with combined PET/CT images, which were changed into X, Y, and Z values in all data sets as the same values ($4.7 \times 4.7 \times 3.3$ mm) for segmentation with the accumulated volume of interest (VOI) manually. Texture analysis was performed using Local Images Features extraction (LIFEx) software (version 6.00, IMIV, CEA, Inserm, CNRS, Univ. Paris-Sud, Université Paris Saclay, CEA-SHFJ, Orsay, France) according to a previous study [12]. PET/CT images were analyzed by two investigators in consensus. The VOIs of the multiple POR/M-OSCCs were obtained, and the SUV_{max} based on the most active tumor metabolism was determined (Fig. 2). Then, the lesion with the highest SUV_{max} was employed for the further analyses.

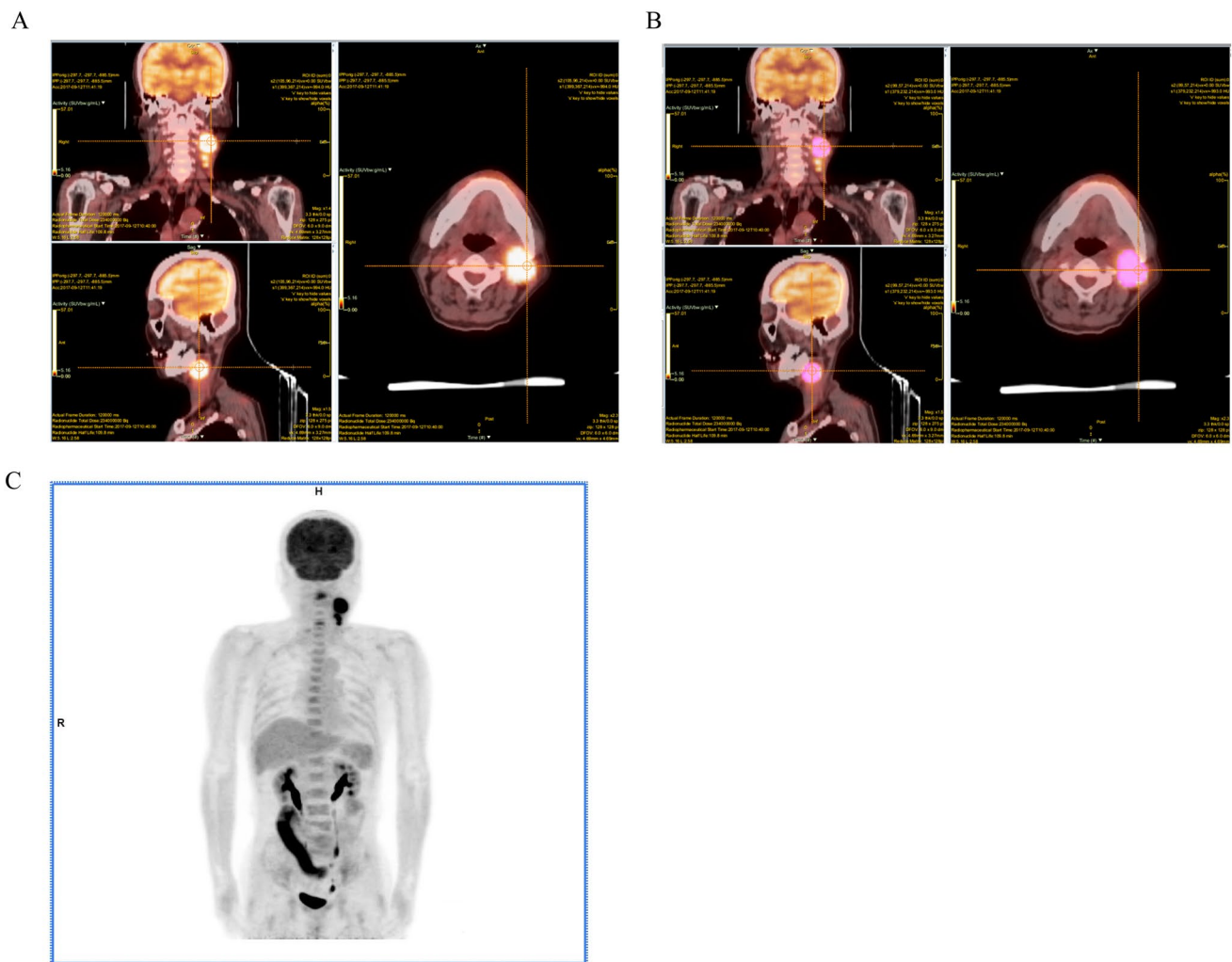


Fig. 2 An example of POR/M-OSCC VOI that was selected using the LIFEx the three-dimensional. A; original PET/CT uptake in POR/M-OSCC lesion B; segmentation for POR/M-OSCC VOI sample. C; Maximum intensity projection (MIP) PET images in non-responder case

VOIs were resampled in 64 bins between 0 and 40 SUV units [13, 14].

The parameters included conventional ones (SUV_{max} , SUV_{min} , SUV_{mean} , SUV_{peak} , SUV_{std} , and TLG), first order (histogram and shape), and second order (gray-level co-occurrence matrix [GLCM], neighborhood gray-level different matrix [NGLDM], gray-level run-length matrix [GLRLM], and gray-level zone-length matrix [GLZLM], and so on). The MTV was calculated using the MTV protocol in LIFEx. All the texture features were summarized in Table 1.

Treatment regimen for POR/M-OSCC combination therapy with cetuximab

Since the study time point was from 2013 to January 2020, NCCN Guidelines version 1.2018 of principles of systemic therapy was employed. The regimens were as follows:

cetuximab plus radiotherapy as per the Bonner trial [15] cetuximab plus cisplatin and 5-FU as per the EXTREME trial [16] and cetuximab plus paclitaxel [17, 18]. Cetuximab was administered at a dose of 400 mg/m^2 for the first regimen and 250 mg/m^2 weekly after first cetuximab administration.

Clinical follow-up and tumor response

RECIST1.0 [19] TNM staging was used to classify the UICC 2009 TNM cancer staging system (8th Edition of the TNM Classification of Malignant Tumors) during the data collection. According to RECIST1.0, tumors were classified as follows: complete response (CR), the disappearance of all target and non-target lesions; partial response (PR), reduction of 30% in the total largest diameter of target lesions considered as reference of the baseline total longest diameter; progressive disease (PD), increase of 20% in the

Table 1 Texture features

Classification	Features
Conventional indices	SUVmin SUVmean SUVstd SUVmax MTV TLG SUVKurtosis SUVExcessKurtosis SUVSkewness SUVQ1 (Quartiles 1) SUVQ2 (Quartiles 2) SUVQ3 (Quartiles 3)
<i>Discretized indices</i>	DISCRETIZED TLG DISCRETIZED_SUVKurtosis DISCRETIZED_SUVExcessKurtosis DISCRETIZED_SUVSkewness DISCRETIZED_SUVmin DISCRETIZED_SUVmean DISCRETIZED_SUVstd DISCRETIZED_SUVmax DISCRETIZED_SUVQ1 DISCRETIZED_SUVQ2 DISCRETIZED_SUVQ3
<i>First-order features</i>	
Histogram based	HISTO_Skewness HISTO_ExcessKurtosis HISTO_Kurtosis HISTO_Entropy_log10 HISTO_Entropy_log2 HISTO_Energy
Shape based	SHAPE_Sphericity SHAPE_Compacity SHAPE_Volume (mL) SHAPE_Volume (voxels) SHAPE_Surface
Second order features (PET and CT)	
Grey-level co-occurrence matrix (GLCM)	GLCM_Homogeneity GLCM_Energy GLCM_Contrast GLCM_Correlation GLCM_Entropy_log10 GLCM_Entropy_log2 GLCM_Dissimilarity
Grey-level run-length matrix (GLRLM)	GLRLM_SRE (Short-Run Emphasis) GLRLM_LRE (Long-Run Emphasis) GLRLM_LGRE (Low Grey-level Run Emphasis) GLRLM_HGRE (High Grey-level Run Emphasis) GLRLM_SRLGE (Short-Run Low Grey-level Emphasis) GLRLM_SRHGE (Short-Run High Grey-level Emphasis) GLRLM_LRLGE (Long-Run Low Grey-level Emphasis)

Table 1 (continued)

Classification	Features
Neighbourhood grey-level difference matrix (NGLDM)	GLRLM_LRHGE (Long-Run High Grey-level Emphasis)
	GLRLM_GLNU (Grey-Level Non-Uniformity)
	GLRLM_RLNU (Run Length Non-Uniformity)
	GLRLM_RP (Run Percentage)
Grey-level zone-length matrix (GLZLM)	NGLDM_Coarseness
	NGLDM_Contrast
	NGLDM_Busyness
	GLZLM_SZE (Short-Zone Emphasis)
	GLZLM_LZE (Long-Zone Emphasis)
	GLZLM_LGZE (Low Grey-level Zone Emphasis)
	GLZLM_HGZE (High Grey-level Zone Emphasis)
	GLZLM_SZLGE (Short-Zone Low Grey-level Emphasis)
	GLZLM_SZHGE (Short-Zone High Grey-level Emphasis)
	GLZLM_LZLGE (Long-Zone Low Grey-level Emphasis)
	GLZLM_LZHGE (Long-Zone High Grey-level Emphasis)
	GLZLM_GLNU (Grey-Level Non-Uniformity)
	GLZLM_ZLNU (Zone Length Non-Uniformity)
	GLZLM_ZP (Zone Percentage)

total largest diameter of target lesions considered as reference of the smallest sum longest diameter recorded since the start of treatment or appearance of new measurable or nonmeasurable lesions or unequivocal progression of existing non-target lesions; SD, in between PR and PD. The best treatment response was the best effect recorded from the start of cetuximub treatment to disease progression based on the pretreatment baseline image according to RECIST. The patients were divided into two groups, the CR + PR (responder) and PD + SD (non-responder) groups, based on the best treatment response during cetuximub therapy from RECIST.

Statistical analysis

All statistical analyses were performed using the R software (<https://www.r-project.org/>, version 3.6.1). The heatmap was generated using the “pheatmap” package, and data were normalized using the z-score before analysis (R Kolde—R package version, 2012). The correlation heatmap was plotted using the “corrplot” package (T Wei, V Simko—R package version 0.73, 2013). The Mann–Whitney U test was used to assess differences in PET texture features between the responder and non-responder. Receiver operating characteristic (ROC) curves were created to determine the optimal cutoff values for discrimination with high accuracy based on the area under the curve (AUC). The correlation analysis between each parameter was performed using the Pearson’s correlation test. In all tests, $p < 0.05$ was considered statistically significant.

Results

The clinical characteristics of all 14 patients are shown in Table 2. The POR/M-OSCC lesions were most commonly found in the lymph nodes of all patients.

Among 65 PET features examined, $SHAPE_{Volume(vx)}$, $SHAPE_{Volume(mL)}$, MTV, and $GLRLM_{RLNU}$ were significantly different between the responder and non-responder groups (Fig. 3). The mean value of TLG in the responder group was lower than that in the non-responder group, but not significant (Table 3). The results of ROC analysis (Fig. 4) revealed that $GLRLM_{RLNU}$ (AUC = 0.917) showed the highest discriminating power between the responder and non-responder groups. The correlation heatmap represented the Pearson’s correlation coefficients (R) of the PET imaging feature (Fig. 5). The inset showed the correlation coefficient value (r) of PET features, and the cutoff values for positive or negative correlations with PET features were set at 1 and –1, respectively. Among the PET features, $SHAPE_{Volume(vx)}$, $SHAPE_{Volume(mL)}$, MTV, and $GLRLM_{RLNU}$ were shown to be significantly correlated with each other ($p < 0.05$, $r > 0.6$).

Figure 6 showed the hierarchical heat map and PET features. The heat map was displayed from red to white and blue from high to low. Hierarchical clustering arranged features with similar tendencies. In the list, the responders were shown in blue and the non-responders in red. The features of the non-responders tended to be highly correlated with features below the heat map. Conversely, in the responders, the lower part of the heat map tended to be blue. Regarding the classification of extraordinary amounts, $GLRLM_{RLNU}$, $SHAPE_{Volume(mL)}$,

Table 2 Patient characteristics (14 patients with metastatic oral cancer treated with cetuximab)

Variables	All patients (n = 14)
<i>POR/M-OSCC*</i>	
Age (median, quartile)	70.0 (58.0–78.0)
<i>Gender, n</i>	
Male	10
Female	4
<i>Site of primary tumor</i>	
Tongue	7
Maxillary	3
Buccal mucosa	1
Floor of mouth	1
Mandibular	2
<i>SCC differentiation</i>	
Well-differentiated	5
Well-moderately differentiated	3
Moderately differentiated	5
Moderate–severely differentiated	1
<i>Target lesion</i>	
Lymph node	6
Lung metastasis	2
Bone metastasis	1
Submandibular metastasis	1
Clavicle	1
Ethmoidal sinus	1
Maxilla metastasis	2
<i>Stage</i>	
II/III/IVA	5/1/8
<i>Regimen</i>	
Cmab + RT	5
Cmab + PTX	5
Cmab + FP	4
Term starting from Cmab to metastasis	28.0 (12.0–65.0)
Term postoperatively from Cmab	314.5 (224.5–477.3)

*Postoperative recurrent or metastatic oral squamous cell carcinoma

Cetuximab (Cmab)

Radiation therapy (RT)

Paclitaxel (PTX)

5-FU plus Cisplatin (FP)

SHAPE_{Volume(vx)} and MTV were recognized in the same cluster. Through the heat map and cluster analysis, the relationship between these features was visually confirmed.

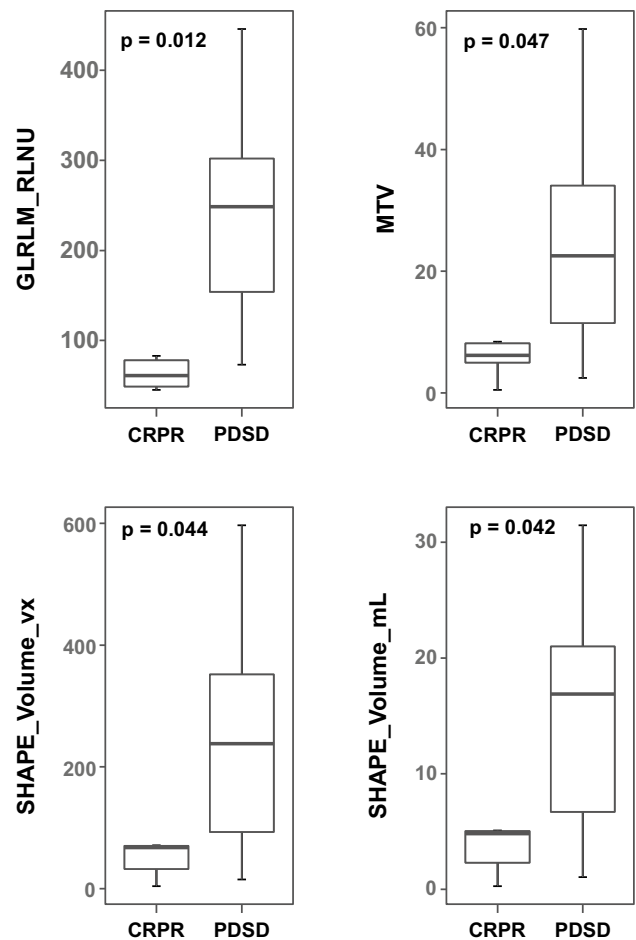


Fig. 3 Univariate analysis using the Mann–Whitney U test for the significance with texture feature between the responders and non-responders with tumor effective in cetuximab-treated patients

Discussion

The present study showed a significant difference between the responder and non-responder groups with respect to the GLRLM_{RLNU}, MTV, SHAPE_{Volume(mL)}, and SHAPE_{Volume(vx)}; all these parameters were volume parameters rather than the conventional two-dimensional parameters (such as SUV_{max}). No significant between-group difference was observed with respect to any of the conventional SUV values; we believe that these results are likely attributable to tumor heterogeneity, since the SUV_{max} reflects just the highest tumor uptake on two-dimensional images. Previous studies have widely used SUV parameters as indices reflecting volume and metabolism and demonstrated their prognostic relevance, with high reproducibility of SUV_{max}. However, use of SUV parameters in the context of head and neck cancer has certain limitations; studies have shown that volume parameters of FDG-PET can better predict the prognosis compared with SUV parameters in these patients [20, 21]. Therefore,

Table 3 Comparison of PET features and ROC curve analysis for differentiation between responders and non-responders ($n = 14$)

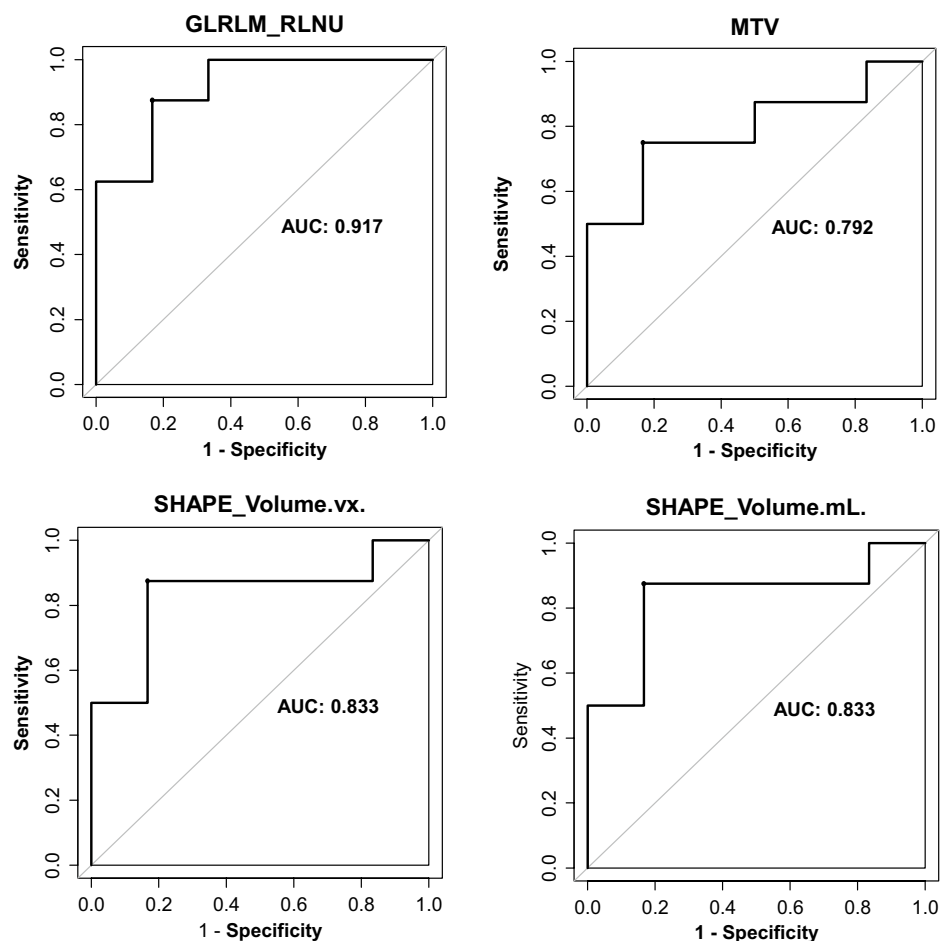
Variables	Responder ($n=6$) mean	Non- responder ($n=8$) mean	p value*	AUC	95% CI	Cutoff
MTV	7.9	24.3	0.047	0.79	0.54–1.00	11.0
TLG	26.1	71.8	0.066	0.79	0.52–1.00	38.2
GLRLM_RLNU	82.9	241.8	0.012	0.92	0.77–1.00	85.1
SHAPE_Volume (mL)	5.5	15.4	0.042	0.83	0.60–1.00	5.71
SHAPE_Volume (vx)	76.8	254	0.044	0.83	0.60–1.00	79.5

*Mann–Whitney U test

Responder: complete response (CR) and partial response (PR)

Non-responder: stable disease (SD) and progressive disease (PD)

ROC receiver operating characteristic

Fig. 4 ROC curves and AUC in texture parameter. The ROC curve in texture parameter POR/M-OSCC oral cancer treated with cetuximab. GLRLM_{RLNU}, SHAPE_{Volume(mL)}, SHAPE_{Volume(vx)}, and MTV demonstrated the ability to be correlated in distinguishing tumor effect with cetuximab in responders and non-responders. The AUC value for each parameter was shown as 0.92, 0.83, 0.83, and 0.79, respectively

volume parameters may provide more specific information about the intertumoral microenvironment. The MTV and TLG, which have the potential to predict the treatment response, have been provided [22, 23]. MTV represents the active metabolic volume in the tumor, and TLG was calculated by multiplying the tumor volume by the SUVmean of the tumor [24]. Moreover, intratumoral heterogeneity will

affect the SUVmean value. Therefore, TLG showed no statistical significance in relation to tumor heterogeneity.

With regard to the current standard treatment for OSCC, surgery is the first regimen, and postoperative concurrent chemoradiotherapy was widely accepted for at high-risk groups based on surgical pathology [25, 26]. A multicenter retrospective study in Japan reported that cetuximab plus

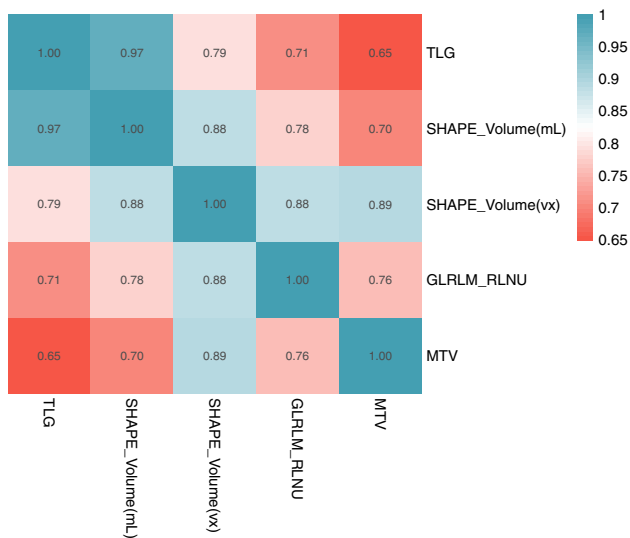


Fig. 5 The triangular heat map representing the Pearson's correlation coefficients of the PET in POR/M-OSCC between texture features. PET imaging features are ordered according to their correlation coefficients angular order of the eigenvectors. The color scale on the right side displays the absolute value of the correlation coefficient. The inset shows the correlation coefficients r value of PET features (the cross was represented as p value of > 0.05)

platinum-based chemotherapy as first-line therapy is an additional option for the systemic treatment for POR/M-OSCC [27]. Thus, evaluating the tumor efficacy of treatment with cetuximab using imaging biomarkers such as PET may be additional information for determining whether to continue the regimen or not.

Despite the small number of patients in this study, we investigated the texture feature (such as the volume parameter of PET) that may influence the antitumor effect. When the threshold is settled in the volume analysis, the VOI margin may be controversial. Texture features, such as GLRLM that represent the number of pixels of run-length and gray-level in the matrix, allow visualization of the margin ranges. Thus, GLRLM could be used to evaluate more velvet margin while setting the threshold for the VOI. In quantitative texture analysis using the functional metabolic structure, the intratumoral structure and heterogeneity have been shown to correlate with image contrast, brightness, and concentration distribution. Texture analysis has been shown to reflect the

tissue-level structural heterogeneity of primary lesions [28]. Our results suggest that texture analysis may be useful not only for evaluating tumor heterogeneity or the histological subtype, but also for predicting the response to molecular-targeted drug therapies.

In this study, we performed a texture analysis of highest accumulation lesion with POR/M-OSCC using PET: it showed a significant difference in the antitumor effect and displayed the morphological pixel value histogram in the tumor and amount of spatial distribution heterogeneity. Some important factors, such as $GLRLM_{RLNU}$, were observed in the texture whereas some factors were not found to be related to the pathological tissue or molecular biology information in this study. Therefore, the relationship between further imaging biomarkers and the antitumor effect must be confirmed in future studies. Moreover, the relationship between EGFR expression and FDG accumulation should be re-examined by adding case, histopathological, and molecular biological information.

The limitation of this study was that the number of patients was small, evaluated as one index using the tumor metabolism of various lesions and the standardization of algorithms and construction of databases were controversial. In the future studies, unnecessary minute quantities not related to machine learning or actual tumor metabolism should be identified. Another limitation was drawing the PET accumulation with POR/M-OSCC by manual VOI. Lastly, recent understanding that recurrent, metastasis, or locally advanced oral cancer molecular-targeting regimen has offered new therapeutic possibilities such as pembrolizumab [29]. The treatment regimen for molecular-targeted drugs was expected to continuously change; however, evaluation of tumor lesions with imaging for each period in cancer therapy may not be changed.

Conclusion

Volumetric parameters of the texture analysis ($GLRLM_{RLNU}$, MTV, $SHAPE_{Volume(vx)}$, and $SHAPE_{Volume(mL)}$) were useful to predict the cetuximab treatment response in POR/M-OSCC. Among them $GLRLM_{RLNU}$ has a better potential for predicting the POR/M-OSCC response.

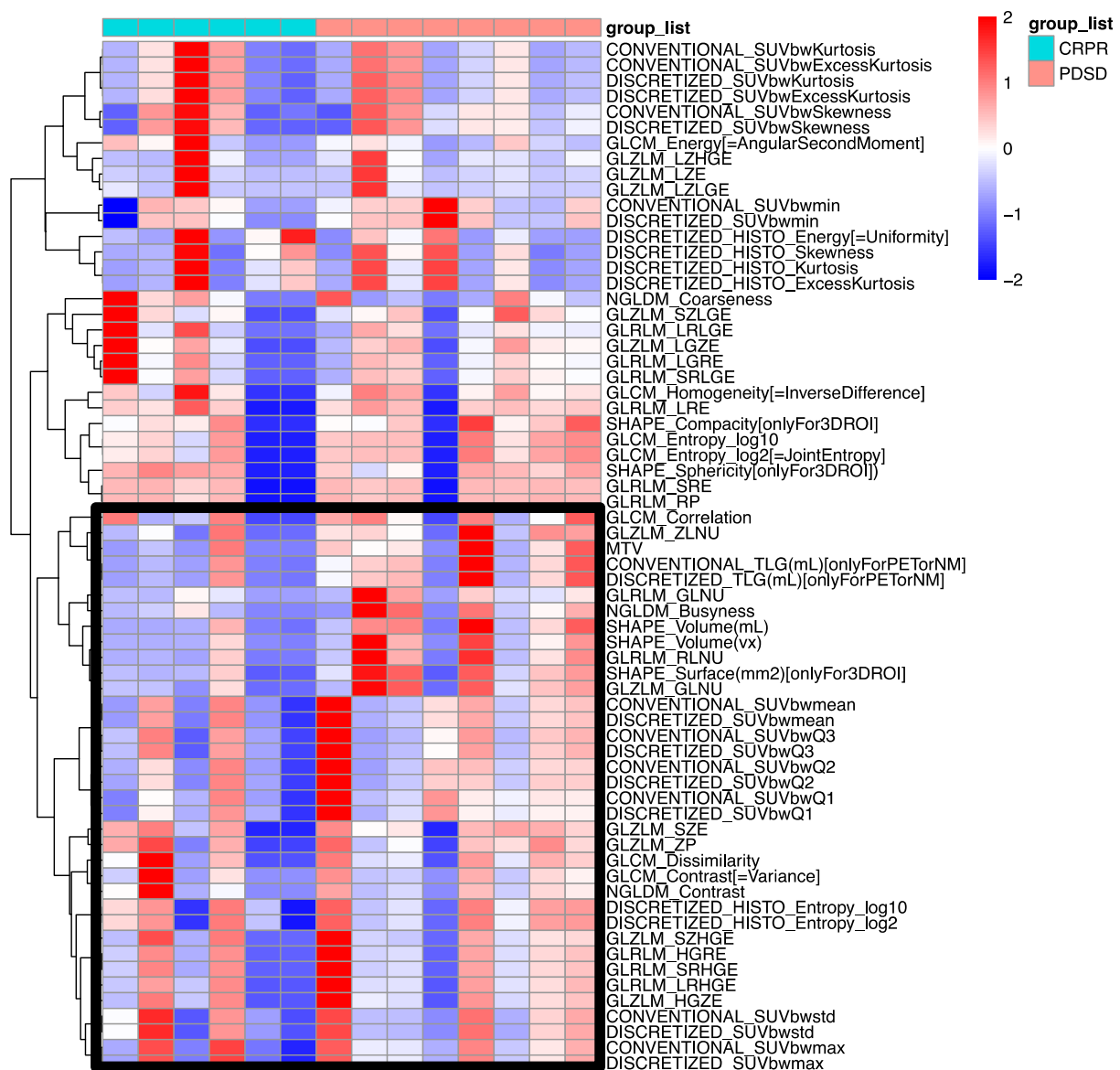


Fig. 6 Radiomics heatmap with responders and non-responders. The figure shows a dendrogram of the heat map and PET features. The heat map is displayed from red to white and blue from high to low. Hierarchical clustering arranges features with similar tenden-

cies nearby on the y-axis. Each patient corresponds to the X-axis. In the Group list, non-responders are shown in red and responders are shown in blue

Sources of funding The study was funded by JSPS KAKENHI with grant number JP 18K17023.

Declarations

Conflict of interest No potential conflicts of interest were disclosed.

Ethics approval and consent to participate The study protocol was approved by the Ethics Committee of our institution. The study was conducted in compliance with the current revision of declaration of Helsinki guideline.

References

1. Adelstein D, MI G, Pfister DG, Spencer S, Adkins D, Brizel DM, et al. Nccn guidelines insights: head and neck cancers, Version 2.2017. *J Natl Compr Canc Netw*. 2017;15:761–70.
2. Wa M, Dj A. Targeting egfr in colorectal cancer. *N Engl J Med*. 2008;359:1834–6.
3. Lk L, Xy J, Xx Z, Dm W, XI S, Hb J. Upregulation of vimentin and aberrant expression of e-cadherin/beta-catenin complex in oral squamous cell carcinomas: correlation with the clinicopathological features and patient outcome. *Mod Pathol*. 2010;23:213–24.
4. Kunkel M, Reichert TE, Benz P, Lehr HA, Jeong JH, Wieand S, et al. Overexpression of glut-1 and increased glucose metabolism

- in tumors are associated with a poor prognosis in patients with oral squamous cell carcinoma. *Cancer*. 2003;97:1015–24.
5. Ahomadegbe JC, Barrois M, Fogel S, Le Bihan ML, Douc-Rasy S, Duvallard P, et al. High incidence of P53 alterations (mutation, deletion, overexpression) in head and neck primary tumors and metastases; absence of correlation with clinical outcome. frequent protein overexpression in normal epithelium and in early non-invasive lesions. *Oncogene*. 1995;10:1217–27.
 6. Avissar M, Mcclean MD, Kelsey KT, Marsit CJ. MicroRNA expression in head and neck cancer associates with alcohol consumption and survival. *Carcinogenesis*. 2009;30:2059–63.
 7. Hoffmann TK, Schuler PJ, Laban S, Grässlin R, Beer M, Beer AJ, et al. Response evaluation in head and neck oncology: definition and prediction. *Orl J Otorhinolaryngol Relat Spec*. 2017;79:14–23.
 8. Parks SK, Chiche J, Pouysségur J. Disrupting proton dynamics and energy metabolism for cancer therapy. *Nat Rev Cancer*. 2013;13:611–23.
 9. Warburg O. On respiratory impairment in cancer cells. *Science*. 1956;124:269–70.
 10. Chicklore S, Goh V, Siddique M, Roy A, Marsden PK, Cook GJ. Quantifying tumour heterogeneity in 18f-fdg pet/ct imaging by texture analysis. *Eur J Nucl Med Mol Imaging*. 2013;40:133–40.
 11. Na KJ, Choi H. Tumor metabolic features identified by 18f-fdg pet correlate with gene networks of immune cell microenvironment in head and neck cancer. *J Nucl Med*. 2018;59:31–7.
 12. Nioche C, Orlhac F, Boughdad S, Reuzé S, Goya-Outi J, Robert C, et al. Lifex: a freeware for radiomic feature calculation in multimodality imaging to accelerate advances in the characterization of tumor heterogeneity. *Cancer Res*. 2018;78:4786–9.
 13. Kim M, Achmad A, Higuchi T, et al. Effects of intratumoral inflammatory process on 18f-fdg uptake: pathologic and comparative study with 18f-fluoro- α -methyltyrosine Pet/Ct in oral squamous cell carcinoma. *J Nucl Med*. 2015;56:16–21.
 14. Kim M, Higuchi T, Nakajima T, Andriana P, Hirasawa H, Tokue A, et al. F-Fdg and ¹⁸f-fam pet-derived metabolic parameters predict outcome of oral squamous cell carcinoma. *Oral Radiol*. 2019;35:308–14.
 15. Bonner JA, Harari PM, Giralt J, Azarnia N, Shin DM, Cohen RB, et al. Radiotherapy plus cetuximab for squamous-cell carcinoma of the head and neck. *N Engl J Med*. 2006;354:567–78.
 16. Vermorken JB, Mesia R, Rivera F, Remenar E, Kawecky A, Rottey S, et al. Platinum-based chemotherapy plus cetuximab in head and neck cancer. *N Engl J Med*. 2008;359:1116–27.
 17. Hitt R, Irigoyen A, Cortes-Funes H, Grau JJ, García-Sáenz JA, Cruz-Hernandez JJ. Phase II study of the combination of cetuximab and weekly paclitaxel in the first-line treatment of patients with recurrent and/or metastatic squamous cell carcinoma of head and neck. *Ann Oncol*. 2012;23:1016–22.
 18. Péron J, Ceruse P, Lavergne E, Buiret G, Pham BN, Chabaud S, et al. Paclitaxel and cetuximab combination efficiency after the failure of a platinum-based chemotherapy in recurrent/metastatic head and neck squamous cell carcinoma. *Anticancer Drugs*. 2012;23:996–1001.
 19. Eisenhauer EA, Therasse P, Bogaerts J, Schwartz LH, Sargent D, Ford R, et al. New response evaluation criteria in solid tumours: revised recist guideline (Version 1.1). *Eur J Cancer*. 2009;45:228–47.
 20. Abd El-Hafez YG, Moustafa HM, Khalil HF, Liao CT, Yen TC. Total lesion glycolysis: a possible new prognostic parameter in oral cavity squamous cell carcinoma. *Oral Oncol*. 2013;49:261–8.
 21. Mk C, Hs J, Yi S, Yk So, Gy P, Jy C, et al. Metabolic tumor volumes by [18f]-fluorodeoxyglucose Pet/Ct correlate with occult metastasis in oral squamous cell carcinoma of the tongue. *Ann Surg Oncol*. 2009;16:3111–7.
 22. Maffione AM, Ferretti A, Grassetto G, et al. Fifteen different 18f-Fdg Pet/Ct qualitative and quantitative parameters investigated as pathological response predictors of locally advanced rectal cancer treated by neoadjuvant chemoradiation therapy. *Eur J Nucl Med Mol Imaging*. 2013;40:853–64.
 23. Hj Im, Yk K, Yi K, Jj L, Ww L, Se K. Usefulness Of combined metabolic-volumetric indices of (18)F-Fdg Pet/Ct for the early prediction of neoadjuvant chemotherapy outcomes in breast cancer. *Nucl Med Mol Imaging*. 2013;47:36–43.
 24. Pinho DF, King B, Xi Y, Albuquerque K, Lea J, Subramaniam RM. Value of intratumoral metabolic heterogeneity and quantitative. *Ajr Am J Roentgenol*. 2020;214:908–16.
 25. Bernier J, Domenge C, Ozsahin M, Matuszewska K, Lefèbvre JL, Greiner RH, et al. Postoperative irradiation with or without concomitant chemotherapy for locally advanced head and neck cancer. *N Engl J Med*. 2004;350:1945–52.
 26. Cooper JS, Pajak TF, Forastiere AA, Jacobs J, Campbell BH, Saxman SB, et al. Postoperative concurrent radiotherapy and chemotherapy for high-risk squamous-cell carcinoma of the head and neck. *N Engl J Med*. 2004;350:1937–44.
 27. Yanamoto S, Umeda M, Kioi M, Kirita T, Yamashita T, Hiratsuka H, et al. Multicenter retrospective study of cetuximab plus platinum-based chemotherapy for recurrent or metastatic oral squamous cell carcinoma. *Cancer Chemother Pharmacol*. 2018;81:549–54.
 28. Tsujikawa T, Rahman T, Yamamoto M, Yamada S, Tsuyoshi H, Kiyono Y, et al. F-Fdg pet radiomics approaches: comparing and clustering features in cervical cancer. *Ann Nucl Med*. 2017;31:678–85.
 29. Sf P, Ka G, Mm G, Cj S, Mm L, Sc M, et al. Safety and efficacy of pembrolizumab with chemoradiotherapy in locally advanced head and neck squamous cell carcinoma: a phase Ib study. *J Clin Oncol*. 2020;38:2427–37.

Publisher's Note Springer Nature remains neutral with regard to jurisdictional claims in published maps and institutional affiliations.